Journal of Materials Chemistry C

Accepted Manuscript

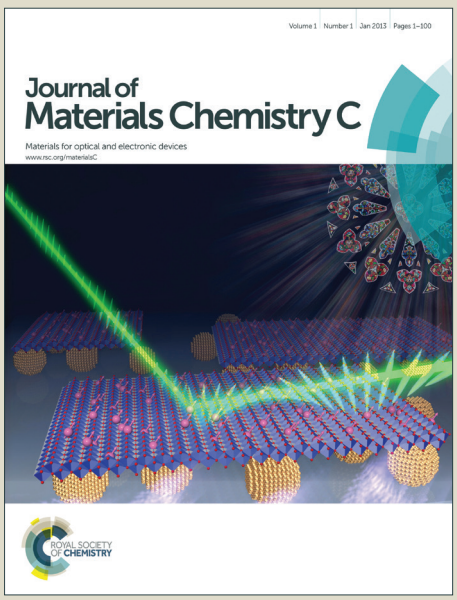

ROYAL SOCIETY OF CHEMISTRY

www.rsc.org/materialsC

Lamellar Nickel hydroxy-halides: Anionic Exchange Synthesis, Structure Characterization and Magnetic behavior.

Mostafa Taibi[a], Noureddine Jouini[a,*], Pierre Rabu[b], Souad Ammar[c], and Fernand Fiévet[c].

[a] Laboratoire des Sciences des Procédés et des Matériaux, LSPM UPR 3407 UPR – CNRS 9001, Institut Galilée, Université Paris 13, PRES Sorbonne Paris Cité 99 av. J. B. Clément, 93400 Villetaneuse, France.

[b] Institut de Physique et Chimie des Matériaux de Strasbourg and Labex NIE, IPCMS UMR7504 CNRS-UDS, 23, rue du Loess BP43 Strasbourg cedex 2, France; Fondation icFRC International Center for Frontier Research in Chemistry, 8, allée Gaspard Monge F-67000 Strasbourg France

[c] ITODYS, Université Paris Diderot Sorbonne Paris Cité, CNRS UMR-7086, Rue Jean-Antoine de Baïf, Paris 75205 France

Corresponding author (email): jouini@univ-paris13.fr

Abstract

Nickel-layered hydroxy-halides LHS-Ni-X (X = Cl, Br, I) have been prepared by exchange reactions conducted in an aqueous medium under inert gas and starting from the parent nickel-layered hydroxyacetate. The latter was prepared by hydrolysis reaction conducted in a polyol medium. IR and X-Ray diffraction (XRD) studies show a total exchange. These compounds exhibit the Brucite-like structure with a turbostratic nature. Their interlamellar distance varies linearly with the radius of the halide anion in the range 7.9 – 8.7 Å while the hydroxyacetate interlamellar distance is 10.53 Å. In comparison with the acetate ion which replaces hydroxyl groups in the Brucite-like layer, EXAFS and XRD investigations show that halide ions are intercalated in the interlayer space along with water molecules without any covalent bond to the nickel ion. All compounds have similar structural features and can be considered as α-type nickel hydroxides, α-$Ni(OH)_2$. These compounds present a ferromagnetic character. The latter is discussed on the basis of the Drillon-Panissod model of ferromagnetic layers interacting via dipole interactions and taking into account the structural features established by XANES and XRD studies along with the intrinsic properties of the halide anions.

Introduction:

Layered Hydroxide Salts (LHS) with the general formula $M^{II}(OH)_{2-x}X_x \cdot nH_2O$ (X= anion like nitrate or carboxylate, M = Ni, Co, Cu, Zn) have been the subject of intensive study in the past decade[1-13], especially due to their peculiar anionic exchange properties[12, 14-16] which result in original tunable functional materials in various fields including electrodes in alkaline cells[17, 18], magnetism[3, 8, 19-33], magneto-optics [34, 35], photovoltaics[36], pressure induced transitions[32], drug delivery,[37] sensors[38, 39] and which are also precursors of functional oxides as well[40-42]. The main synthesis route for these compounds consists in the neutralization of an aqueous solution of nitrate or acetate salt by a base such as sodium hydroxide or ammonia. The reaction needs accurate pH control and bubbling of inert gas to avoid metal oxidation and the presence of carbonate anion in the final product, due to the atmospheric CO_2. An alternative route used to obtain Co, Ni and Zn layered hydroxides consists in the hydrolysis of acetate salts dissolved in a polyol medium[5]. All compounds obtained using this route have a similar general formula and exhibit layered structures but belong to different structural types. The nickel hydroxysalts LHS-Ni-X obtained via the polyol route are isostructural with the Brucite mineral $Mg(OH)_2$ which has a hexagonal layer structure made up of edge sharing $Mg(OH)_6$ octahedra. The structure of zinc hydroxysalts LHS-Zn-X usually derives from that of the hydrozincite compound, which consists in the stacking of Brucite-type sheets in which one-quarter of the octahedral cationic sites are unoccupied. This sheet is sandwiched between two layers formed by zinc ions in tetrahedral sites which are placed above and below each octahedral vacancy. Zinc hydroxychloride $Zn_5(OH)_8Cl_2 \cdot 1H_2O$[43]and zinc hydroxynitrate $Zn_5(OH)_8(NO_3)_2 \cdot 2H_2O$[44] are prototypical examples of this triple-deck slab type. The structural type adopted by the cobalt hydroxysalts depends on the nature of the anion X. The cobalt hydroxynitrate is isotructural with the Brucite[28]. Similar layered structures with Co(II) ions in octahedral sites only were obtained with benzene- or monothiophene-dicarboxylate anions,[14, 45] while the hydroxyacetate and several hydroxysalts (sulfates, alkylsulfonates, alkanedioates, thiophenecarboxylates, cyclohexane-dicarboxylate, chloride…) exhibit the hydrozincite-like structure.[5, 14, 46-49] As mentioned above, the layered hydroxysalts show interesting anionic exchange properties regardless of the nature of the bonding between metal cation and the X anion. Indeed, the nitrate or acetate anions are readily exchanged by a variety of organic or inorganic anions. These anions are inserted between the layers and thus govern the interlayer

spacing which can be varied on a wide scale from 7 to 41 Å.[10, 19, 25, 26, 33, 49] A noteworthy characteristic of these compounds concerns their magnetic properties in relation with the structure of the metal hydroxide sheets and the interlayer distances. The magnetic behavior of cobalt and copper hydroxysalts has been thoroughly investigated. When the interlayer distance is smaller than 10 Å, an antiferromagnetic order is observed due to exchange interactions occurring between layers through the small inserted anions (nitrate or acetate) and hydrogen bonds. Conversely a 3D ferromagnetic order can be observed when the interlayer distance is larger than 10 Å due to the occurrence of dipole interaction between ferromagnetic layers with a perpendicular easy axis .[50, 51] The ordering temperature, T_C, for a given metal cation appears to be slightly dependent on the interlayer distance, the ordering temperature being mainly governed by the divergence of the correlation length within the planes. For instance, when grafting alkylcarboxylates in between the layers, copper (II) hydroxysalts exhibit an interlayer spacing ranging from 29 to 40 Å and are ferromagnetic with $19 \leq T_C \leq 21$ K. The cobalt (II) analogues have $16.5 \leq T_C \leq 22.7$ K as the interlayer spacing varies from 9.3 to 27.4 Å.[25, 26]

The same feature was also observed for nickel (II) hydroxysalts. Indeed 3D ferromagnetic order occurs at almost constant T_C ($16 \leq T_C \leq 18$ K) as the interlayer spacing varies from 7.5 to 31.7 Å.[33, 46, 52] These magnetic studies essentially focused on phases with large interlayer distances (d_{001}>10 Å) resulting from the insertion/grafting of long alkyl chain organic spacers with the general formula $C_nH_{2n+1}X$ (X stands for sulfate, sulfonate or carboxylate).

Reports on the magnetic properties of nickel hydroxysalts with interlayer distances smaller than 10 Å are quite scarce. They concern essentially hydroxynitrates or hydroxysilicates, showing antiferromagnetic (metamagnetic) or ferromagnetic behaviors.[29, 53, 54]

Here we report the use of halides as spacers which enabled us to prepare nickel hydroxysalts with the general formula $Ni(OH)_{2-x}X_x \cdot nH_2O$ (X = Cl, Br, I) with d_{001}< 10 Å. These materials exhibit ferromagnetic behavior despite small interlayer distances. This rather unexpected feature will be tentatively explained on the basis of the nature of the halide-nickel bond and the nature of magnetic interactions occurring within and between the layers via these highly polarizable anions.

2. Experimental

2.1. Sample preparation

The hydrated nickel acetate, halide salts (NaCl, KBr, KI) and diethyleneglycol were purchased from Prolabo or Fluka and used without any further purification.

2.1.1. LHS-Ni-OAc preparation : The nickel hydroxyacetate LHS-Ni-OAc was prepared following the method described by Poul et *al*.[5] It consists of the hydrolysis at 172°C of nickel acetate tetrahydrate dissolved in diethyleneglycol (0.1 M). As discussed elsewhere, the precipitation of LHS-Ni-OAc occurred, as in the sol gel method, via hydrolysis and inorganic polymerization reactions.[55]

2.1.2. LHS-Ni-X (X = Cl, Br and I) preparation: 0.4 g of nickel(II) hydroxyacetate (LHS-Ni-OAc) was stirred in 200 ml of an aqueous solution (0.02 M) containing the appropriate salt (NaCl, KBr, KBr) for one day at room temperature to form nickel(II) hydroxyhalides, LHS-Ni-X (X = Cl, Br, I). The pH increased to 8.5 due to the release of acetate. The procedure was repeated twice to complete the exchange. The products were washed three times with alcohol, separated from the solution by centrifugation, and then dried under nitrogen at room temperature. In order to avoid the presence of CO_3^{2-} in the solution and accordingly in the final product, water was boiled before use to remove dissolved CO_2 and the exchange was conducted under nitrogen bubbling. Furthermore, the products were dried and kept in plastic vials under nitrogen atmosphere.

2.2. Chemical analysis

Carbon and hydrogen elemental analysis was performed at the Centre d'analyse de l'Université Pierre et Marie Curie. Nickel was titrated by EDTA using alcoholic dithizone as an indicator. The acetate amount of the parent compound was determined by ion chromatography using a DIONEX DX-100 ion chromatograph fitted with AG-4 and AS4-SC columns. The halide/Ni ratio was estimated by Energy dispersive X-ray spectroscopy using Leica Stereoscan 440 microscope (probe diameter: 200 nm).

2.3. Characterization

Powder X-ray diffraction (XRD) patterns were obtained at room temperature using a Siemens D5000 diffractometer with Cu-$K_{\alpha 1}$ radiation (λ=1.5406 Å). Temperature dependent XRD was carried out between 20-400 °C using a Phillips PW1050 diffractometer with rodhied platinum as sample holder. The crystallite size was calculated using the Scherrer equation.

X-Ray absorption spectra at the Ni-K edge were measured at 10 K in the transmission mode at station D42 at the LURE-DCI storage ring (Orsay, France), using a Si(111) channel-cut crystal monochromator and two ion chambers as detectors. EXAFS data were analyzed using the "EXAFS pour le Mac" software package.[56] The first and second shells (Ni-O and Ni-Ni) were fitted using theoretical backscattering amplitude and phase shift functions for absorber-backscatter atomic pairs calculated in the structural model of β-$Ni(OH)_2$ using the FEFF 7 code.[57] Electron microscopy and diffraction studies were performed on a JEOL-100 CX II microscope. Differential thermal and thermogravimetric analyses (DTA and TGA) were carried out on a Setaram TG 92-12 thermal analyzer with a 1°C/mn heating rate under air, in an alumina crucible. Infrared spectra were recorded by transmission on an Equinox 55 spectrometer on pressed KBr pellets with 4 cm^{-1} resolution.

The magnetic measurements on microcrystalline samples enclosed in a gel capsule were carried out in the temperature range 2 to 300 K in AC and DC modes using a Quantum Design SQUID magnetometer "MPMS–5S". Thermal variation of the DC-susceptibility was collected at 200 Oe and the field dependence of the DC magnetization was measured in a field range of -50 kOe – 50 kOe , at a temperature of 2 K. Thermal variation of the AC-susceptibility was conducted at 2 and 20 Hz with an alternating field of 10 Oe .

3. Results and discussion

3.1. Chemical composition

The chemical composition of all the hydroxyhalides is similar (Table 1). The X/Ni (X = Cl, Br, I) ratio is lower than the acetate ratio (OAc/Ni) in the parent compound. As will discussed below, IR and XRD analyses clearly indicate complete exchange of acetates in part by halide and in part by hydroxide since the exchange was conducted in a basic medium (pH = 8.5). This feature has been previously observed on layered hydroxysulfonates obtained by a similar method.[33] The chloride content in LHS-Ni-Cl is close to that observed in similar compounds previously prepared by cathodic reduction[58] or by precipitation with NaOH.[59] It should be noted that a small amount of carbon, compared to that found in acetate, is still present in the exchanged products LHS-Ni-X (1.60 - 1.84 %). This is mainly due to the presence of adsorbed polyol traces, as will be discussed in the Infrared study section. Such adsorption appears to be a common feature of inorganic compounds obtained in a polyol medium.[5, 60]

The chemical formula in Table 2 was deduced from chemical analysis and TGA analysis. Table 2 also indicates the amount of adsorbed polyol in the final products. This amount has

been included into to the chemical formulas to calculate the theoretical weight loss (See SUPP INFO 1). The as-obtained total weight losses are in keeping with those observed by TGA analysis taking into account that NiO is the final product of decomposition as shown by X-ray diffraction analysis.

3.2. Infrared study

The IR spectrum of the parent compound LHS-Ni-OAc (Figure 1) shows intense bands at 1600 and 1380 cm^{-1} assigned to $\nu_{as}(-COO^-)$ and $\nu_a(-COO^-)$ respectively. The difference between the two bands ($\nu_{as}-\nu_a = 220\ cm^{-1}$) is characteristic of unidentate acetate ligand.[61-63]
The anion exchange by halide is clearly indicated by the disappearance of the characteristic bands of the acetate, as shown in Figure 1. All IR spectra show a broad peak at high frequency, in the range 3580-3400 cm^{-1}, assigned to hydroxyl groups and water molecules.
The lower frequency band around 3400 cm^{-1} corresponds to water and the band at higher frequency (around 3570 cm^{-1}) is due to the hydroxyl groups weakly bonded with intercalated species (H_2O, Anions).[14, 64] The peak around 1620 cm^{-1} is due to $\delta(H_2O)$ vibration of the water molecules interacting with the meatl ions. At low frequency (700 - 400 cm^{-1}) there are two bands corresponding to δ(OH) (620 cm^{-1}) and ν(NiO) (470 cm^{-1}) vibrations. One can note that the intensities of hydroxyl and water vibration bands depend on the amount of water present in the compound. The higher is the amount of water, the higher is the band intensity. The three samples LHS-Ni-X (X = Cl, Br, I) along with parent LHS-Ni-OAc (Figure.1) exhibit two weak bands around 1000 cm^{-1} characteristic of adsorbed polyol . For LHS-Ni-X (X = Cl, Br, I) two other weak peaks are observed in the range 1300 – 1500 cm^{-1} and they can be due to the presence of a small amount of the carbonate CO_3^{2-} group.

3.3. Thermal analysis

The TGA curves of hydroxyhalides are shown in Figure 2. Several weight losses were observed. The first loss (7.44 - 10.64 %) occurring in the temperature range 40 - 150°C is due to the departure of adsorbed and intercalated water. The second weight loss (8.50-26.68 %) occurring in the temperature range 150–350°C is assigned to the decomposition and dehydroxylation of hydroxide sheets. The LHS-Ni-I shows one additional weight loss (18.43 %) in the temperature range 350-500°C. The final product of thermal decomposition was found to be NiO in all cases. In the case of LHS-Ni-I, the decomposition seems not complete at 500°C while X-Ray diffraction of the corresponding calcined samples indicates only the

presence of NiO. This means that some adsorbed or amorphous species such as hydrogen iodide remain on the NiO particles. A similar behavior was reported by Theiss et *al* in the case of the decomposition of LDH ZnAl-I.[65]

3.4. X-ray diffraction study

XRD patterns for the four samples are shown in Figure 3. They exhibit symmetrical 00*l* reflection at low 2θ and two (hk0) dissymmetrical reflections at high 2θ (around 33.6 and 59.9°/ Cu-$K_{\alpha 1}$). This type of pattern has been previously observed in LHS-Co, LHS-Cu, LHS-Zn, suggesting turbostratic disorder in the stacking of the layers. [1, 5, 14, 33]

The shift towards high 2θ of the (00*l*) reflections in the hydroxyhalides compared to hydroxyacetate confirms the exchange of the acetate by halide anions resulting in materials with smaller interlayer spacing. The XRD patterns can be indexed based on the hexagonal cell of a brucite-like lattice, with one slab per cell. The lattice parameter *a*, corresponding to the Ni-Ni distance within the layer, remains almost constant (3.09(1) Å) in all compounds. Conversely, the interlayer spacing (*c* parameter) increases from 7.93 (LHS-Ni-Cl) to 8.60 Å (LHS-Ni-I) as the radius of the intercalated ion increases (Table 3). The variation of the interlayer spacing follows the linear relationship c = 4.46 + 1.9*r* where *r* is anionic radii (Figure 4). From this relation, it can be concluded that the interlayer spacing depends only on the halide size. The value for r = 0 (c = 4.46 Å) is close to the interlayer spacing of β-$Ni(OH)_2$ phase which is 4.61 Å.[66] The correlation length along c deduced from the XRD analysis, in table 3, indicates that the crystallites consist in the stacking of ca 10 monolayers. The crystallites are thus not really nanosheets but rather "nano-multilayers.

It is interesting to note that the interlamellar distances in the present LHS-Ni-X (Cl, Br, I) (7.93 – 8.60 Å) are greater than those of Botallackite, Atacamite or the hexagonal type $Ni_2(OH)_3X$ reported by Oswald and Feitknecht (5.51 – 6.41 Å) in which the halogen is assumed to occupy OH sites after topotactic exchange.[67] Distances are very similar however to those observed for LDH-Zn-Cr-X or LDH-Mg-Al-X (7.45 – 8.29 Å).[68-70] This suggests that the halide anions and part of water molecules are likely located, as in LDH compounds, in the center of the inter-slab space and do not replace the hydroxyl groups in the inorganic layers. The X-Ray diffraction patterns are in keeping with this hypothesis. Indeed the I(002)/I(001) intensity ratio increases with the electronic density of the halide (Table 3). A similar behavior was observed when carbonate is exchanged by oxometalate (V, W, Mo) anions in LDH-Ni-Co.[71, 72] In this case simulations of the XRD patterns with the DIFFaX program and the EXAFS study have clearly established that this inversion is due to the location of molybdate

or tungstate in the center of the inter-layer space.[73] As will be shown hereafter EXAFS studies of the compounds presented in this paper also confirm that halide anions are not directly linked by a iono-covalent bond to nickel ion.

3.5. Transmission Electron Microscopy

Figure 5 presents Transmission Electron Microscopy (TEM) pictures of LHS-Ni-Cl as an example of the series. The TEM micrograph is characteristic of morphology of turbostatic particles which consists of aggregates of thin crumpled sheets. The electron diffraction pattern confirms the hexagonal symmetry of the sheets as found in the Brucite-like structure.

3.6. Temperature resolved X-ray diffraction

The XRD patterns recorded at temperatures range 20-400°C under air are given in Figure 6 . The layered structure of LHS-Ni-I is stable up to 200°C and that of the chloride and bromide derivatives are stable up to 250°C. For all compounds the (00*l*) reflections shift towards higher 2θ values indicating a decrease of interlayer distance as the temperature increases from 20 to 200 – 250 °C (1.43Å ≤ Δd_{001} ≤ 1.62 Å).). A decrease in intensity and a broadening of the (00*l*) reflection lines is concomitantly observed.

It suggests an increase of disorder in the layer's stacking probably due to the departure of water molecules, as shown by the TGA analysis. Between 150 and 250°C the compounds do not exhibit any significant evolution of interlayer distance. LHS-Ni-Cl and LHS-Ni-Br are more stable than LHS-Ni-I which decomposed at 200°C. For all compounds the decrease of the interlayer spacing associated with the dehydration process is smaller than the water molecular diameter (2.8 Å). This suggests that water molecules are not forming independent layers but more probably lay in a disordered mixed H_2O/X layer between the nickel hydroxide sheets.

3.7. X-Ray Absorption Spectroscopy

The modulus of the Fourier transform (FT) of the total EXAFS signal at the Ni-K edge is shown in Figure 7 for the whole series. There are no significant differences between the FT of LHS-Ni-OAc and that of LHS-Ni-X, X = Cl, Br and I. For all compounds, two main peaks localized at 1.6 and 2.7 Å (without phase shift correction) are assigned to the first and the second atomic neighbor shells around nickel ions.

There is no shift of the R-position of the hydroxy-halide compounds compared to the hydroxy-acetate, in which nickel is firstly coordinated by six oxygen atoms and secondly by six nickel atoms. This suggests that all these compounds adopt the same Brucite-like structure

in which halide ions are not replacing hydroxyl groups and thus are not coordinated to nickel atoms by iono-covalent bond. The results of the fitting procedure, assuming single diffusion processes on the inverse Fourier transformed EXAFS signal of these two peaks, are given in SUPP INFO 2 and Table 4.

The analysis shows that the first Ni-O shell consists effectively only of almost six oxygen atoms – the uncertainty of the coordination number is usually estimated to be about 15% –[56] at a distance of 2.05 Å, close to the number reported on the oxygen octahedral environment of nickel in $Ni(OH)_2$ [74, 75] and $Ni_{0.80}Zn_{0.39}(OH)_2(CH_3\ COO)_{0.39}\cdot 0.92H_2O$ [7] compounds. This feature is similar to that occurring in LDH compounds. Indeed a pure oxygen environment of Cr and Zn has clearly been established by EXAFS studies in the case of LDH-Zn-Cr-Cl. [76]
Thus, for this LHS-Ni-X series, the EXAFS spectroscopy and X-Ray diffraction studies indicate that the halide anions and water molecules are in the same layer within the interlamellar space corresponding to the (002) plane.
All these results allow us to propose a structural model for LHS-Ni-X (X=Cl, Br, I). It is compared to that of LHS-Ni-A where A is an alkylsulfonate with a long alkyl chain in Figure 8. All compounds, i.e. the present nickel layered hydroxy-halides and the alkylsulfonate analogues, have similar structural features and can be considered as α-type nickel hydroxides, α-$Ni(OH)_2$, according to Genin et *al.*[77] and Rajamathi et *al.*[78]. α-$Ni(OH)_2$ is the second allotropic form of nickel hydroxide beside the more stable phase β-$Ni(OH)_2$. The latter exhibits a basal spacing of 4.6 Å.[66] The two forms crystallize in the layered hexagonal $Mg(OH)_2$ structure with the c axis being larger in the α-phase. Starting from the β-phase, it is possible to replace hydroxyl groups by different anions with variable size. The α-$Ni(OH)_2$ compounds are formed when the anions do not substitute completely the hydroxyl anions but are intercalated in between the layers. In that case, the negative charge of the inserted anions is balanced by hydroxyl vacancies in the layers. Depending on the inserted anion, the interlamellar distance varies in a large range up to 40 Å.[33, 49]

3.8. Magnetic properties

The main magnetic characteristics of the nickel hydroxy-halides and hydroxy-acetate parent compounds are presented in Table 5, with that of LHS-Ni-Alkysulfonates for comparison.[33] The temperature dependence of the DC-susceptibility, $\chi(T)$, and its inverse, $\chi^{-1}(T)$, measured

in the temperature range 4 - 300 K, with an applied field H of 200 Oe is plotted in Figure 9. At high temperature all compounds follow the Curie-Weiss law ($1/\chi = (T-\theta)/C$). The linear fit of $\chi^{-1} = f(T)$ in the 150-300 K temperature range, gave a positive θ value $16 \leq \theta \leq 23$ K, indicating that intra-plane ferromagnetic interactions dominate as for the hydroxy-acetate analogue ($\theta = 27$ K).

The calculated values of the Curie constant C ($C = Ng^2\mu^2_B S(S+1)/3k$, with S=1) and the corresponding g factor values (Table 5) are in keeping with those expected for octahedral nickel (II).[79]

The $\chi T(T)$ curves for all prepared samples are presented in Figure 10. At low temperatures χT increases significantly to reach a high maximum value in the range 80-200 $K.cm^3.mol^{-1}$ related to in-plane ferromagnetic correlations. The temperature at the maximum of χT increases from 12 K for iodide to 21 K for chloride. All compounds show a hysteresis loop of M(H) measured at 2 K(Figure 11) in keeping with the occurrence of a long range ferromagnetic order. It was noticed above that particles consist of aggregates of thin crumpled sheets. Thus, one could also envisage that uncompensated spins at the surfaces of the nanosheets could contribute to stabilize a net moment even if the compounds would manifest a 3D antiferromagnetic order. This explanation can be ruled out however. Indeed, the compounds studied here have not been subject to exfoliation process and thus their crystallites are constituted of several nanosheets as discussed above. Moreover, would the ferromagnetic behavior result from uncompensated spins in an antiferromagnetic system, one would observe very small magnetic moments in the M vs Field curves, which is not the case. Finally, the thermal variation of the magnetization does not indicate any sign of antiferomagnetism. The magnetic behavior is typical of ferromagnetic layers that couple ferromagnetically at lower temperatures, as found in all alpha –$Ni(OH)_2$ systems actually.

Accordingly, the thermal variation of the AC-susceptibilities (Figure 12) shows a peak in the out-of-phase signal χ'' confirming the 3D ferromagnetic ordering of all the present compounds. The position of the peaks in both χ' and χ'' seems not frequency-dependent. It varies however as a function of the intercalated halide. The ordering temperature, chosen at the maximum of $\chi'(T)$, increases from 20 K for LHS-Ni-I to 36 K for LHS-Ni-Cl.

These data indicate that the nickel hydroxy-halides, despite a small interlayer distance, exhibit a 3D ferromagnetic order, contrarily to the antiferromagnetic order usually encountered in hydroxy-nitrate, or -acetate, when interlayer spacing is less than 10 Å.[26, 29, 32, 49] Hence, the present hydroxy-halides show a magnetic behavior similar to the hydroxyacetate and the

nickel hydroxy-alkylsulfonates though the latter exhibit larger interlayer distances.[46] However, some differences can be pointed out. First, the Weiss temperatures, θ, are higher than observed for the alkylsufonate salts, denoting higher divergence of the in-plane correlation length with lowering temperature. Second, the ordering temperature varies with the size of the intercalated halide while it is independent of the anion length, even varying this distance to a large extent, for the alkylsulfonates (Table 5).[33]

According to the Drillon-Panissod model,[50, 51, 80, 81] the overall magnetic behavior of layered compounds built of ferromagnetic layers (like hydroxides) depends on the competition between two types of inter-layer magnetic interactions. The super-exchange interaction via hydrogen bonds and electronic orbital overlap dominates for small interlayer distances, usually leading to an antiferromagnetic ordering.[49, 80, 82] As the interlayer distance is increased by insertion of long spacers, the superexchange interactions vanish in favor of dipole-dipole interactions that become predominant, leading to 3D ferromagnetic order when easy axis is perpendicular to the layers. An antiferromagnetic order is predicted for in-plane easy axis. Drillon and Panissod have clearly shown that the critical temperature T_C, at which the 3D order occurs, is governed mainly by intra-plane interactions expressed by the correlation length ξ. Beyond the case of layers separated by large spacers, the interplane coupling can be controlled by a spin polarization mechanism in bridged systems. Such a situation occurred in layered hydroxides functionalized by various dicarboxylate bridges.[22, 49] In LHS compounds involving small anions (nitrate, chloride, acetate, carbonate), the anions may replace hydroxyl groups as in Botallackite or Gerhardtite-type hydroxo-salts,[4, 28, 29] or can be intercalated between the layers, as in the present exchanged compounds. The in-plane interactions can occur via the anions when they coordinate the metal ions within the layers but are mainly transmitted through the bridging hydroxyl groups as established in the case of copper (II) hydroxysalts.[30, 83]

Regarding the magnetic properties of the $Ni(OH)_2$ derivatives, the data from the literature are often discussed on the basis of the interlamellar distance. β- $Ni(OH)_2$ exhibits the lowest interlamellar distance (d_i = 4.6 Å) and is an antiferromagnet below T_N = 25.5 K with a metamagnetic transition to ferromagnetic state under a threshold field of 55 kOe and 2 K.[84, 85] As stated before, the α-$Ni(OH)_2$ compounds show a 3D ferromagnetic order in keeping with recent reports.[84, 86, 87] The ordering temperature varies in the range 16-23 K in nickel hydroxy-acetate and hydroxy-dodecyl sulfates or sulfonates (d_i up to 30.5 Å).[23, 33, 87] It should be noted that Seehra et al.[87] reported on the synthesis of a lamellar nickel-hydroxyacetate with

a significantly lower interlamellar distance (8.6 Å) in comparison with that presented here (10.53 Å). Despite this difference, the two compounds have a 3D ferromagnetic order with almost similar Tc. In these compounds, the inter-layer ferromagnetic ordering is well explained by the Drillon-Panissod model considering the dipolar interactions as the driving interactions between layers when d_i is higher than ca 10 Å. Within this scheme, the 3D ordering temperature is expected to vary very slightly with the interlayer distance, in keeping with all reported works cited above. Only few compounds have a shorter interlamellar distance as the nickel hydroxyl-halides investigated here. To the best of our knowledge, the only known compounds are LHS-Ni-NO_3. Yet, the magnetic properties of the latter appear to depend on the synthesis method. Indeed, LHS-Ni-NO_3 prepared from LHS-Ni-OAc by exchange reaction, similarly to the LHS-Ni-Halides presented here, exhibits a 3D ferromagnetic order at 17 K with an interlayer distance of 7.5 Å.[33] On the other hand LHS-Ni-NO_3 prepared by co-precipitation or slow hydrolysis exhibits an interlayer period of 6.9 Å and shows a ferromagnetic behavior with a spin-glass or disordered ferromagnetic ground state below 10 K.[29] The former corresponds to the α form whereas the structure of the latter is consistent with a disordered β form.[29] These results highlight the importance of the structure of the nickel hydroxide layers regarding the magnetic behavior of these systems. Actually, our results compared with that found in the literature support this idea.

Moreover, we can notice the influence of the hydroxyl vacancies on the magnetic ordering temperature of the α-$Ni(OH)_2$ compounds. In the title compounds, XRD and EXAFS studies have shown that the halides are located at the center of the interlayer space leading to anionic vacancies within the layers, corresponding to the formulation $(Ni(OH)_{2-x}\square_x)(X_x \cdot nH_2O)$. The presence of such vacancies has also been established in the case of the hydroxyacetate and alkylsulfonate homologues.[33] In that case, the magnetic ordering temperature of 17 K does not vary with the basal spacing (see Table 5), which is fully consistent with the Drillon-Panissod model. Hence, the ordering temperature, T_C, seems to depend mainly on the amount of hydroxyl vacancies in the α-$Ni(OH)_2$ structure. A high amount of vacancies, as observed in the hydroxyacetate (x = 0.50) and alkylsulfonate homologues (x = 0.30), reduces the intra-layer magnetic correlation length and thus leads to low T_C (around 17K). Conversely, the vacancies in the present hydroxyl-halide salts are significantly lower (x = 0.17). This lower amount favors a larger intra-layer magnetic correlation length and hence higher T_C's.

The general magnetic behavior of the α-$Ni(OH)_2$ series is well explained by the concomitant effect of intra-layer magnetic correlation length and inter-layer dipole interactions. Yet, the T_C

of the hydroxy-halide salts varies with the interlayer distance, suggesting a different coupling mechanism. Regarding the interlayer structure and the nature of the anions, alkylsulfonates and alkylsulphates are surfactants with a hydrophilic head and a hydrophobic alkyl group as a tail. In LHS-alkylsulfonates, these features lead to a peculiar arrangement of the organic layers and the water molecules, as illustrated in Figure 8. The hydrophilic groups and water are merely attracted by the inorganic hydroxide layers and the saturated carbon chains separate the magnetic layers by wide distances. In contrast, in the Nickel layered hydroxy-halides, the interlayer distance is small and weak coupling is expected to occur through the ionic interlayer.[88] Moreover, the water and halide anions are in the same medium plane and because of small d values, exchange interactions between planes can occur, possibly relayed by H-bonds favored by the water molecules. The polarizability of halide anions might also play a role. For instance, iodide is a highly polarizable anion favoring exchange through H-bonds. Thus the decrease of T_C from chloride to iodide can be explained by an increase in polarizability,[89] which favors interactions.

Conclusion

Nickel layered hydroxyl-halides LHS-Ni-X (X = Cl, Br, I) have been prepared by anionic exchange reaction starting from LHS-Ni-OAc. The interlamellar distance varies linearly with the halide radius from 7.93 to 8.60 Å from chloride to iodide. X-Ray diffraction and XAS studies show that the halide ions are not linked to nickel cations by an iono-covalent bond but located at the center of the interlayer space together with water as observed for layered double hydroxides (LDH). All structural features support that the present nickel layered hydroxy-halides LHS-Ni-X (X = Cl, Br, I) belong to the α-$Ni(OH)_2$ family of compounds. Despite their small interlamellar distance, the present hydroxy-halide compounds exhibit a 3D ferromagnetic order, whereas it was found previously on series of cobalt and copper analogues that this family of compounds usually presents antiferromagnetic ordering when basal spacing is less than ca 10 Å. This ferromagnetic behavior is in line with the general behavior observed for α-$Ni(OH)_2$ analogues. Yet, contrarily to the nickel layered hydroxy-alkyl-sulfonate or -sulphate series for which T_C is almost independent of the interlamellar distance, this temperature varies slightly with the nature of the halide anion. This can be tentatively explained on the basis of the nature and structural arrangement of the

inserted anions between the magnetic layers and competition between through-anion and dipolar interactions.

Acknowledgements

The authors thank J. Morrice-Abrioux for careful examination of the manuscript and Dr. I. Balti for her help during the preparation of the revised version.

Notes and references

1. J.-H. Choy, Y.-M. Kwon, K.-S. Han, S.-W. Song and S. H. Chang, *Mater. Lett.*, 1998, **34**, 356-363.
2. A. Jiménez-López, E. Rodríguez-Castellón, P. Olivera-Pastor, P. Maireles-Torres, A. A. G. Tomlinson, D. J. Jones and J. Rozière, *J. Mater. Chem.*, 1993, **3**, 303-307.
3. V. Laget, C. Hornick, P. Rabu, M. Drillon, P. Turek and R. Ziessel, *Adv. Mater.*, 1998, **10**, 1024.
4. N. Masciocchi, E. Corradi, A. Sironi, G. Moretti, G. Minelli and P. Porta, *J. Solid State Chem.*, 1997, **131**, 252.
5. L. Poul, N. Jouini and F. Fievet, *Chem. Mater.*, 2000, **12**, 3123-3132.
6. P. Rabu, J.-M. Rueff, Z. L. Huang, S. Angelov, J. Souletie and M. Drillon, *Polyhedron*, 2001, **20**, 1677-1685.
7. R. Rojas, C. Barriga, M. A. Ulibarri, P. Malet and V. Rives, *J. Mater. Chem.*, 2002, **12**, 1071-1078.
8. V. Laget, S. Rouba, P. Rabu, C. Hornick and M. Drillon, *J. Magn. Magn. Mater.*, 1996, **154**, L7.
9. A. van Bommel and J. R. Dahn, *Chem. Mater.*, 2009, **21**, 1500-1503.
10. T. Yamanaka, T. Sako, K. Seki and M. Hattori, *Solid State Ion.*, 1992, **53-56**, 527.
11. P. Li, Z. P. Xu, M. A. Hampton, D. T. Vu, L. Huang, V. Rudolph and A. V. Nguyen, *J. Phys. Chem. C*, 2012, **116**, 10325.
12. R. Rojas, M. A. Ulibarri, C. Barriga and V. Rives, *Appl. Clay Sci.*, 2010, **49**, 176.
13. M. Taibi, S. Ammar, N. Jouini and F. Fiévet, *J. Phys. Chem. Sol.*, 2006, **67**, 932.
14. A. Demessence, G. Rogez and P. Rabu, *Chem. Mater.*, 2006, **18**, 3005-3015.
15. Y. Du and D. O'Hare, *Inorg. Chem.*, 2008, **47**, 11839-11846.
16. S. Hasan, H. A. Ali, M. Al-Qubaisi, M. Z. Hussein, M. Ismail, Z. Zainal and M. N. Hakim, *Int. J. Nanomedicine*, 2012, **7**, 3351.
17. H. Bode, K. Dehmelt and J. Witte, *Zeitschrift für anorganische und allgemeine Chemie*, 1969, **366**, 1-21.
18. X. Liu, R. Ma, Y. Bando and T. Sasaki, *Adv. Mater.*, 2012, **24**, 16.
19. W. Fujita and K. Awaga, *Inorg. Chem.*, 1996, **35**, 1915-1917.
20. W. Fujita and K. Awaga, *J. Am. Chem. Soc.*, 1997, **119**, 4563-4564.
21. W. Fujita, K. Awaga and T. Yokoyama, *App. Clay Sc.*, 1999, **15**, 281-303.
22. C. Hornick, P. Rabu and M. Drillon, *Polyhedron*, 2000, **19**, 259-266.
23. M. Kurmoo, P. Day, A. Derory, C. Estournès, R. Poinsot, M. J. Stead and C. J. Kepert, *J. Solid State Chem.*, 1999, **145**, 452-459.
24. V. Laget, M. Drillon, C. Hornick, P. Rabu, F. Romero, P. Turek and R. Ziessel, *Journal of Alloys and Compounds*, 1997, **262-263**, 423.

25. V. Laget, C. Hornick, P. Rabu and M. Drillon, *J. Mater. Chem.*, 1999, **9**, 169-174.
26. V. Laget, C. Hornick, P. Rabu, M. Drillon and R. Ziessel, *Coord. Chem. Rev.*, 1998, **178-180**, 1533.
27. G. G. Linder, M. Atanasov and J. Pebler, *J. Solid State Chem.*, 1995, **116**, 1.
28. P. Rabu, S. Angelov, P. Legoll, M. Belaiche and M. Drillon, *Inorg. Chem.*, 1993, **32**, 2463-2468.
29. S. Rouba, P. Rabu, E. Ressouche, L.-P. Regnault and M. Drillon, *J. Magn. Magn. Mat.*, 1996, **163**, 365-372.
30. E. Ruiz, M. Llunell, J. Cano, P. Rabu, M. Drillon and C. Massobrio, *J. Phys. Chem. B*, 2006, **110**, 115-118.
31. H. Shimizu, M. Okubo, A. Nakamoto, M. Enomoto and N. Kojima, *Inorg. Chem.*, 2006, **45**, 10240-10247.
32. K. Suzuki, J. Haines, P. Rabu, K. Inoue and M. Drillon, *J. Phys. Chem. C*, 2008, **112**, 19147-19150.
33. M. Taibi, S. Ammar, N. Jouini, F. Fiévet, P. Molinié and M. Drillon, *J. Mater. Chem.*, 2002, **12**, 3238-3244.
34. J.-M. Rueff, J.-F. Nierengarten, P. Gilliot, A. Demessence, O. Crégut, M. Drillon and P. Rabu, *Chem. Mater.*, 2004, **16**, 2933-2937.
35. E. Delahaye, S. Eyele-Mezui, M. Diop, C. Leuvrey, P. Rabu and G. Rogez, *Dalton Trans.*, 2010, **39**, 10577-10580.
36. B. Schwenzer, J. R. Neilson, K. Sivula, C. Woo, J. M. J. Fréchet and D. E. Morse, *Thin Solid Films*, 2009, **517**, 5722.
37. J.-M. Oh, S.-J. Choi, G.-E. Lee, S.-H. Han and J.-H. Choy, *Adv.Func.Mater.*, 2009, **19**, 1617-1624.
38. S. Si, A. Taubert, A. Mantion, G. Rogez and P. Rabu, *Chemical Science*, 2012, **3**, 1945 -1957.
39. A. Khenifi, Z. Derriche, C. Forano, V. Prevot, C. Mousty, E. Scavetta, B. Ballarin, L. Guadagnini and D. Tonelli, *Anal. Chim. Acta*, 2009, **654**, 97.
40. T. Biswick, W. Jones, A. Pacula, E. Serwicka and J. Podobinski, *J. Solid State Chem.*, 2007, **180**, 1171.
41. L. Markov, K. Petrov and A. Lyubchova, *Solid State Ionics*, 1990, **39**, 187-193.
42. W. X. Zhang and K. Yanagisawa, *Chem. Mater.*, 2007, **19**, 2329-2334.
43. R. Allmann, *Z. Kritallogr.*, 1968, **126**, 417.
44. W. Stählin and H. R. Oswald, *Acta Cryst.*, 1970, **B26**, 860-863.
45. Z. L. Huang, M. Drillon, N. Masciocchi, A. Sironi, J. T. Zhao, P. Rabu and P. Panissod, *Chem. Mater.*, 2000, **12**, 2805-2812.
46. M. Kurmoo, P. Day, A. Derory, C. Estournès, R. Poinsot, M. J. Stead and C. J. Kepert, *J. Solid State Chem.*, 1999, **145**, 452-459.
47. M. Kurmoo, H. Kumagai, S. M. Hughes and C. J. Kepert, *Inorg. Chem.*, 2003, **42**, 6709-6722.
48. J. R. Neilson, B. Schwenzer, R. Seshadri and D. E. Morse, *Inorg. Chem.*, 2009, **48**, 11017.
49. G. Rogez, C. Massobrio, P. Rabu and M. Drillon, *Chem. Soc. Rev.*, 2011, **40**, 1031-1058.
50. M. Drillon and P. Panissod, *J. Magn. Magn. Mat.*, 1998, **188**, 93-99.
51. P. Panissod and M. Drillon, in *Magnetism: Molecules to Materials IV (2003), 233-270.*, eds. J. S. Miller and M. Drillon, Wiley-VCH Verlag GmbH & Co. KGaA, Weinheim, Germany, 2003, pp. 233-270.
52. M. Guillot, M. Richard-Plouet and S. Vilminot, *J. Mater. Chem.*, 2002, **12**, 851-857.
53. M. Richard-Plouet and S. Vilminot, *J. Mater. Chem. ,* , 1998, **8**, 131.

54. S. Rouba, *Corrélations structures-propriétés magnétiques dans une série d'hydroxynitrates de métaux de transition 1d et 2d*, Thèse de doctorat, Université Louis Pasteur, Strasbourg, 1996.
55. L. Poul, S. Ammar, N. Jouini, F. Fiévet and F. Villain, *Journal of Sol-Gel Science and Technology*, 2003, **226**, 26&-265.
56. A. Michalowicz, *J. Phys. IV*, 1997, **7**, 235-236.
57. J. Rehr, in *FEFF Project*, Department of Physics, BOX 351560, University of Washington, Seattle, WA 98195-1560; jjr@phys.washington.edu, 1996.
58. G. H. Annal Therese and P. Vishnu Kamath, *J. Appl. Electrochem.*, 1998, **28**, 539.
59. M. Rajamathi, G. N. Subbanna and P. V. Kamath, *J. Mater. Chem.*, 1997, **7**, 2293-2296.
60. V. Prevot, C. Forano and J. P. Besse, *Chem. Mater.*, 2005, **17**, 6695.
61. G. B. Deacon and R. J. Phillips, *Coord. Chem. Rev.*, 1980, **33**, 227-250.
62. C. Dendrinou-Samara, G. Tsotsou, L. V. Ekateriniadou, A. H. Kortsaris, C. P. Raptopoulou, A. Terzis, D. A. Kyriakidis and D. P. Kessissoglou, *J. Inorg. Biochem.*, 1998, **71**, 171-179.
63. K. Nakamoto, *Infrared and Raman Spectra of Inorganic and Coordination Compounds*, Wiley, New York, 1986.
64. F. Kooli, L. C. Chisem, M. Vucelic and W. Jones, *Chem. Mater.*, 1996, **8**, 1969.
65. F. L. Theiss, M. J. Sear-Hall, S. J. Palmer and R. L. Frost, *Desalination and Water Treatment*, 2012, **39**, 166-175.
66. R. W. Cairns and E. Ott, *J. Am. Chem. Soc.*, 1933, **55**, 534-544.
67. H. R. Oswald and W. Feitknecht, *Helv. Chim. Acta*, 1964, **47**, 272 - 289.
68. J. W. Boclair and P. S. Braterman, *Chem. Mater.*, 1998, **10**, 2050.
69. N. Iyi, K. Fujii, K. Okamoto and T. Sasaki, *Appl. Cl. Sc.*, 2007, **35**, 218.
70. R. Rojas Delgado, M. Arandigoyen Vidaurre, C. P. De Pauli, M. A. Ulibarri and M. J. Avena, *J. Colloid Interface Sci.*, 2004, **280**, 431.
71. M. Menetrier, K. S. Han, L. Guerlou-Demourgues and C. Delmas, *Inorg. Chem.*, 1997, **36**, 2441.
72. C. Vaysse, L. Guerlou-Demourgues, A. Demourgues and C. Delmas, *J. Solid State Chem.*, 2002, **167**, 59.
73. C. Vaysse, L. Guerlou-Demourgues, A. Demourgues, F. Lazartigues, D. Fertier and C. Delmas, *J. Mater. Chem.*, 2002, **12**, 1035-1043.
74. J. B. Espinose de la Caillerie, J. B. Kermarec and M. Clause, *J. Am. Chem. Soc.*, 1995, **117**, 11471.
75. K. I. Pandya, W. E. O'Grady, D. A. Corrigan, J. McBreen and R. W. Hoffman, *J. Phys. Chem.*, 1990, **94**, 21.
76. A. De Roy, J. P. Besse and P. Bondot, *Mater. Res. Bull.*, 1985, **20**, 1091.
77. P. Genin, A.Delahaye-Vidal, F. Portemer, K. Tekaia-Elhsissen and M. Figlarz, *Eur. J. Solid State Inorg. Chem.*, 1991, **28**, 505-518.
78. M. Rajamathi, P. Vishnu Kamath and R. Seshadri, *J. Mater. Chem.*, 2000, **10**, 503-506.
79. R. L. Carlin, *Magneto-Chemistry*, Springer-Verlang, Berlin, 1986.
80. P. Rabu and M. Drillon, *Adv. Engin. Mater.*, 2003, **5**, 189-210.
81. E. M. Bauer, C. Bellitto, G. Righini, M. Colapietro, G. Portalone, M. Drillon and P. Rabu, *Inorg. Chem.*, 2008, **47**, 10945-10952.
82. S. Pillet, M. Souhassou, C. Lecomte, P. Rabu, M. Drillon and C. Massobrio, *Phys. Rev. B*, 2006, **73**, 115116.
83. C. Massobrio, P. Rabu, M. Drillon and C. Rovira, *J. Phys. Chem. B*, 1999, **103**, 9387–9391.

84. D. R. James and M. S. Seehra, *J. Phys.: Condens. Matter*, 2012, **24**, 076002.
85. J. D. Rall, M. S. Seehra, N. Shah and G. P. Huffman, *The 41st annual conference on magnetism and magnetic materials*, 2010, **107**, -.
86. H. B. Li, P. Liu, Y. Liang, J. Xiao and G. W. Yang, *CrystEngComm*, 2013, **15**, 4054-4057.
87. M. S. Seehra and V. Singh, *J. Phys.: Condens. Matter*, 2013, **25**, 356001.
88. H. Amouri, C. Desmarets, A. Bettoschi, Marie Noelle, R. K. Boubekeur, P. Rabu and M. Drillon, *Chem.-Eur. J.*, 2007, **13**, 5401-5407.
89. G. Ahn-Ercan, H. Krienke and W. Kunz, *Curr. Opin. Colloid In.*, 2004, **9**, 92.

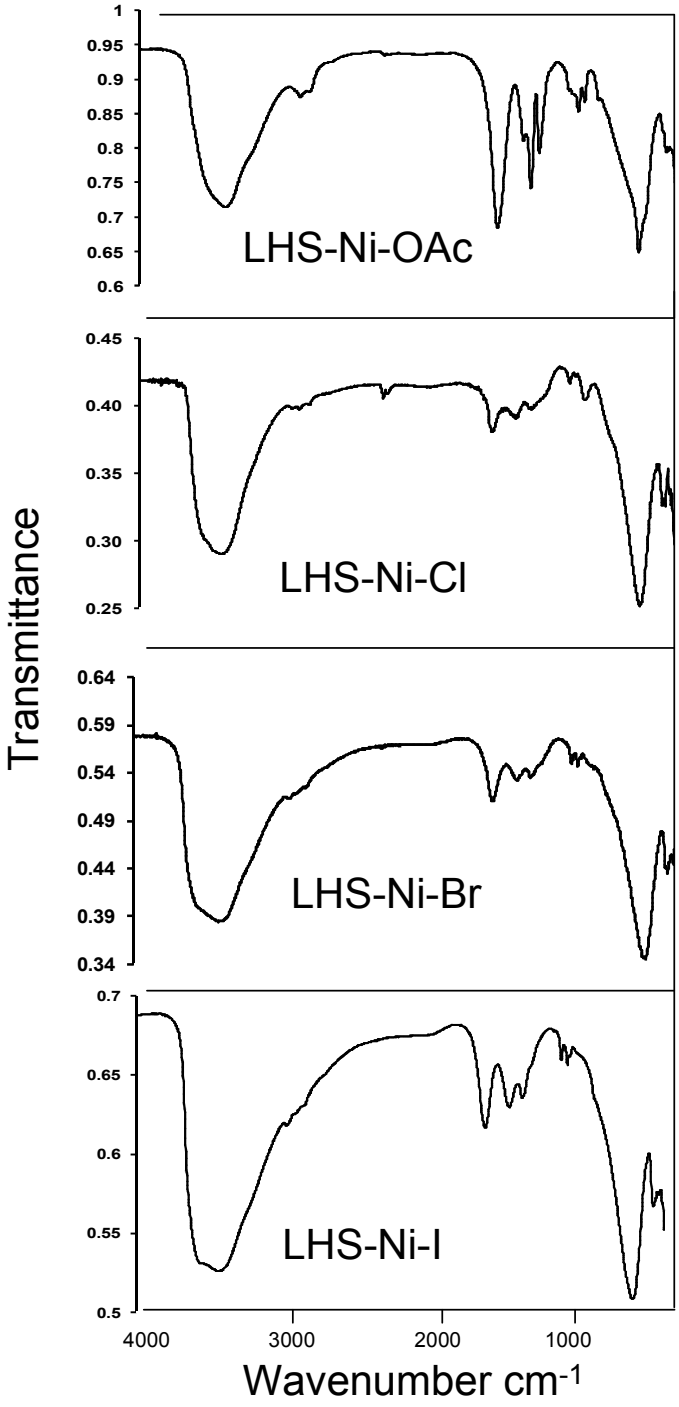

Figure 1: FTIR spectra of LHS-Ni-X compounds (X = OAc, Cl, Br, I)

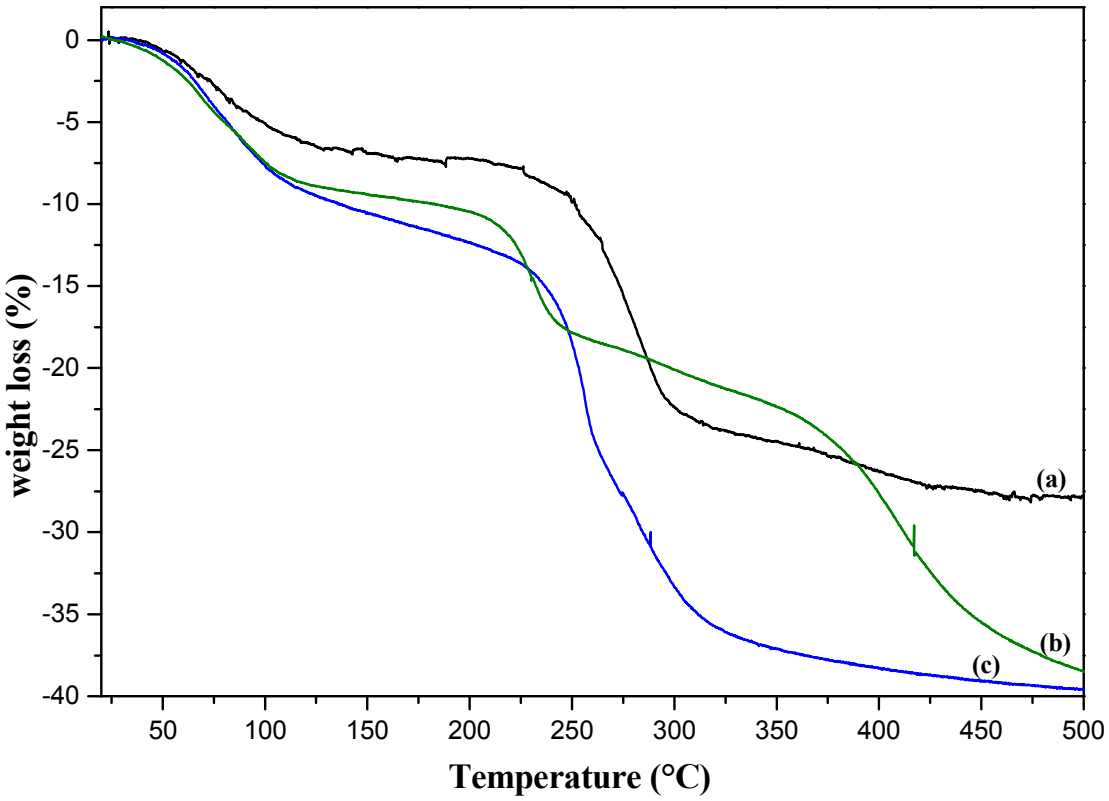

Figure 2: TGA data of (a) LHS-Ni-Cl; (b) LHS-Ni-I and (c) LHS-Ni-Br recorded under air

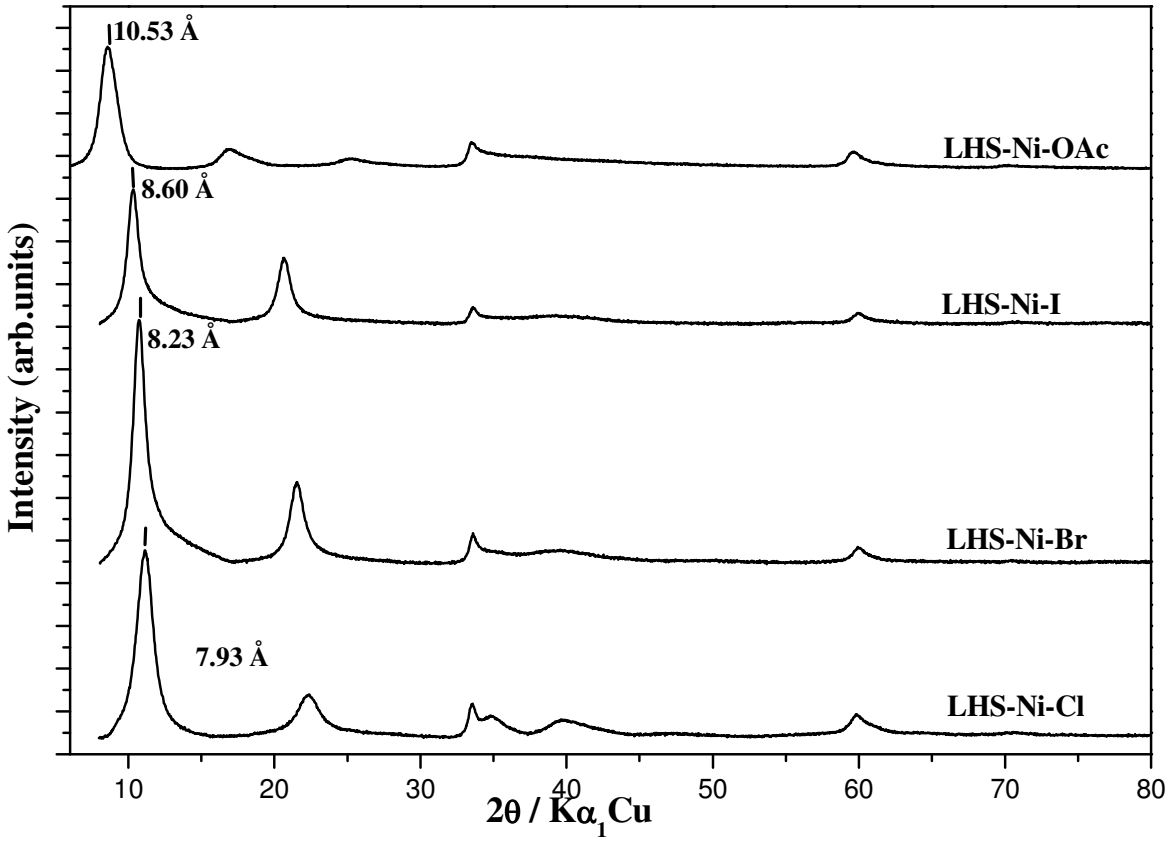

Figure 3: Powder X-ray diffraction patterns of LHS-Ni-X (X = OAc, I, Br, Cl)

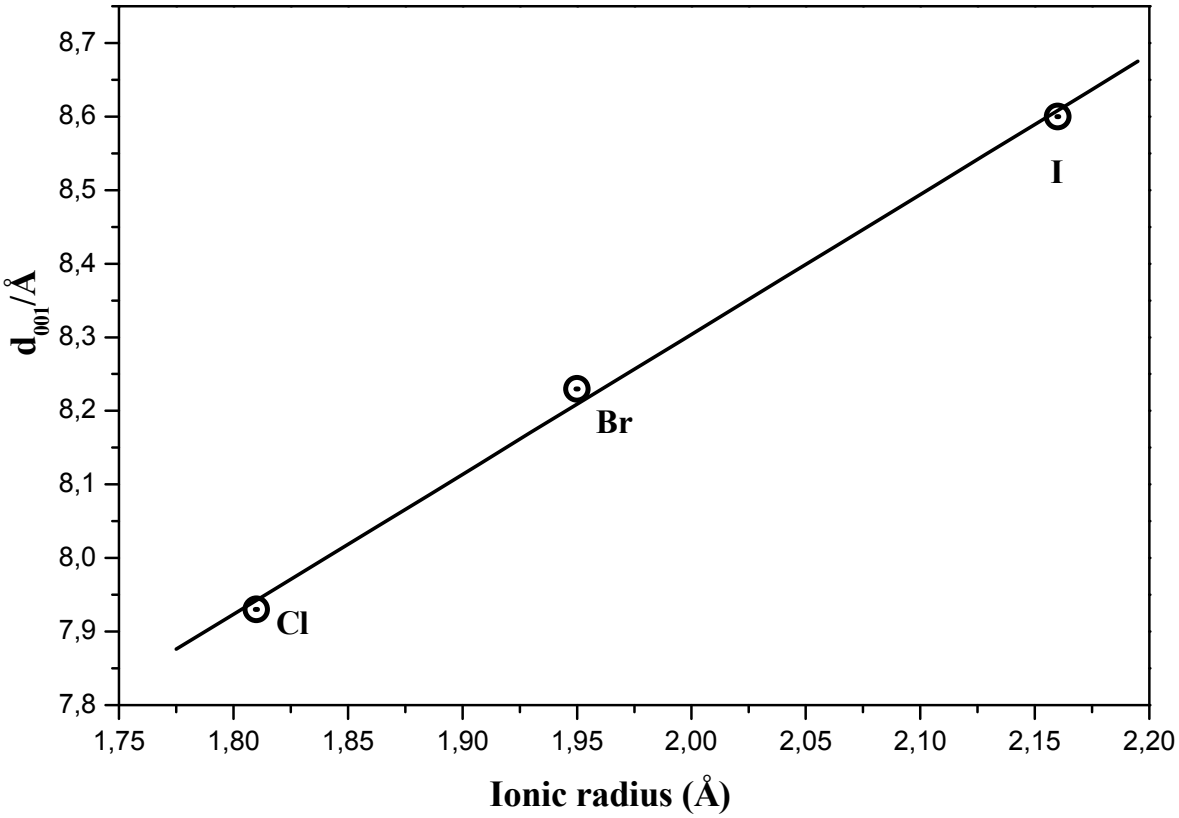

Figure 4: Variation of the basal spacing as function of the ionic radius of the inserted halogen anions for LHS-Ni-X (X = Cl, Br, I)

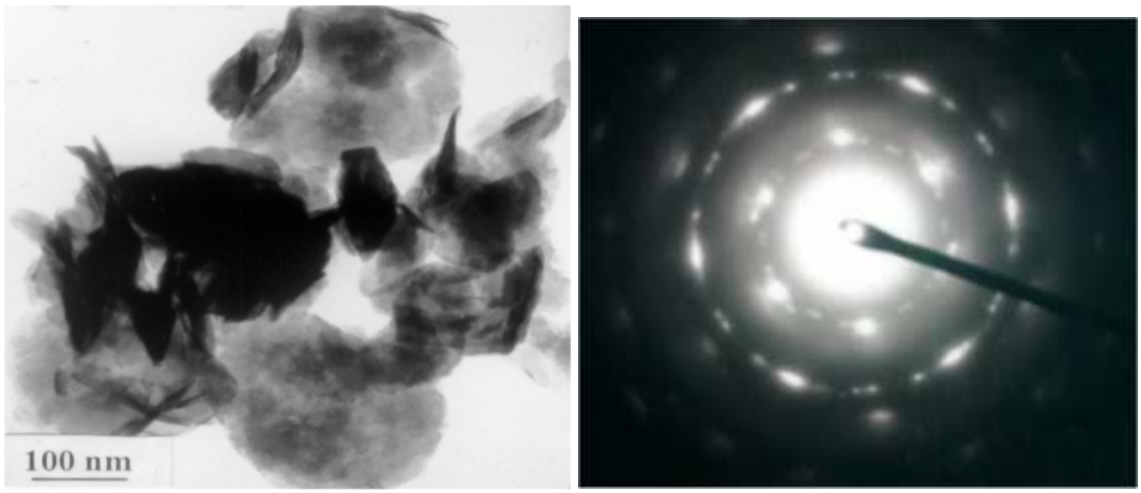

a **b**

Figure 5 : TEM results of LHS-Ni-Cl : (a) Transmission electron micrograph; (b) Electron diffraction pattern.

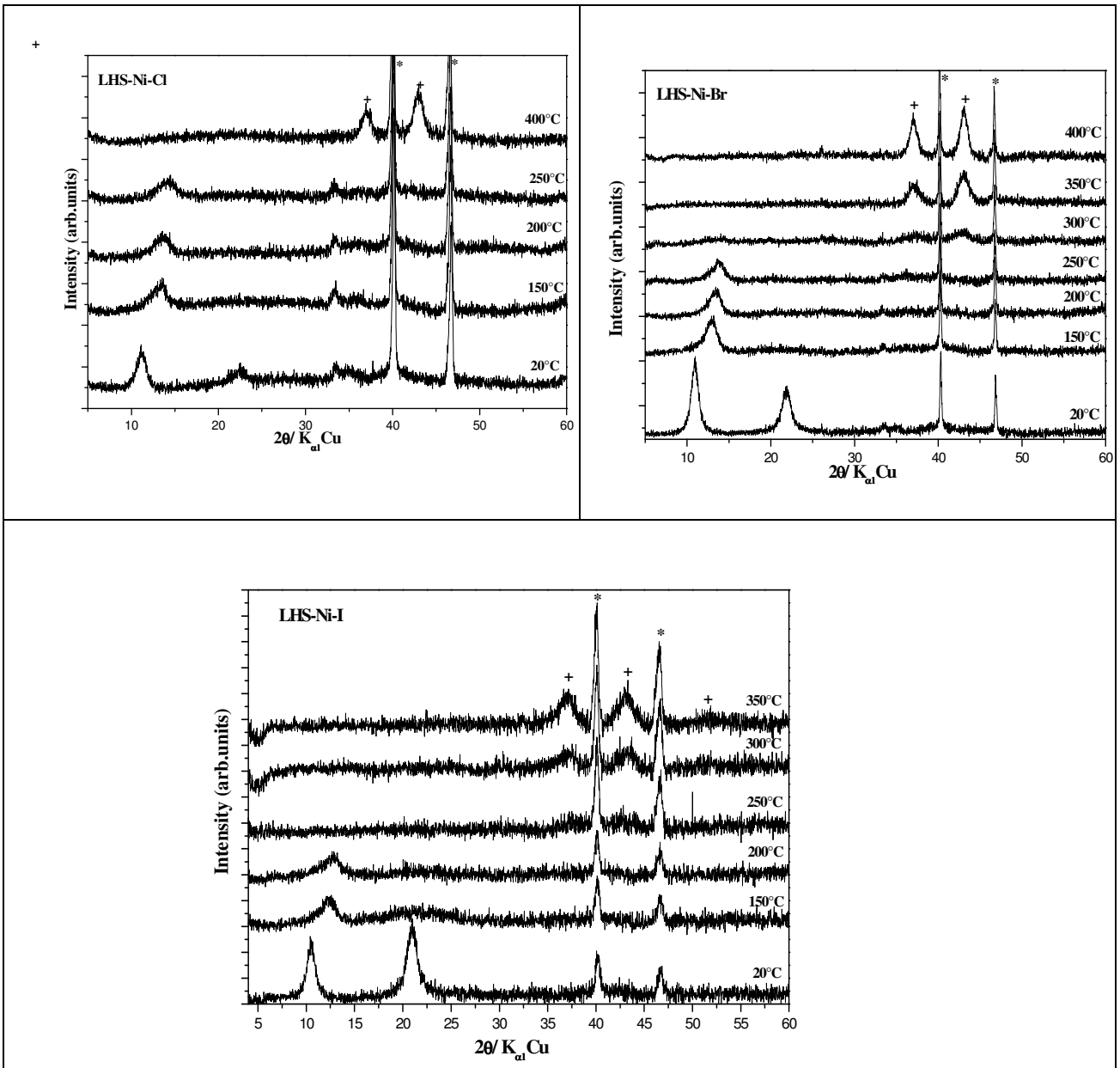

Figure 6: Temperature-solved powder X-ray diffraction patterns of the nickel hydroxyhalides. (+: NiO; *: sample holder.)

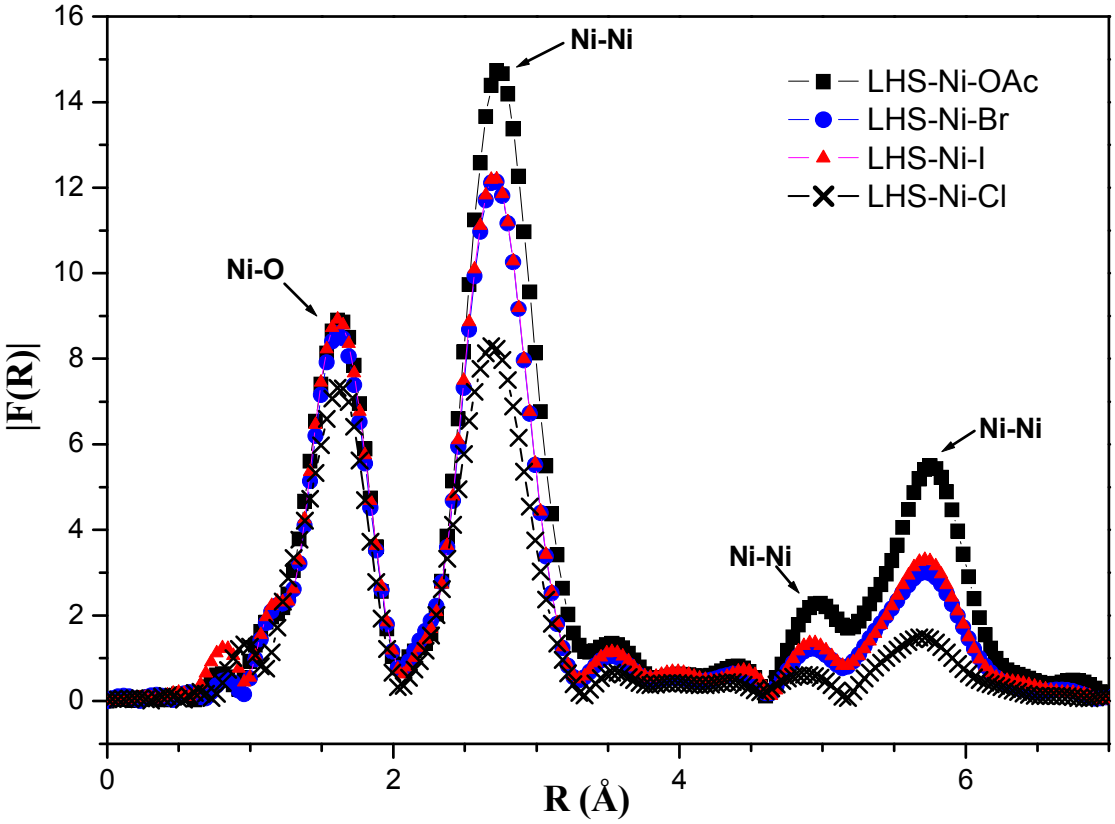

Figure 7: Fourier transforms for Ni-edge spectrum of synthesis compounds.

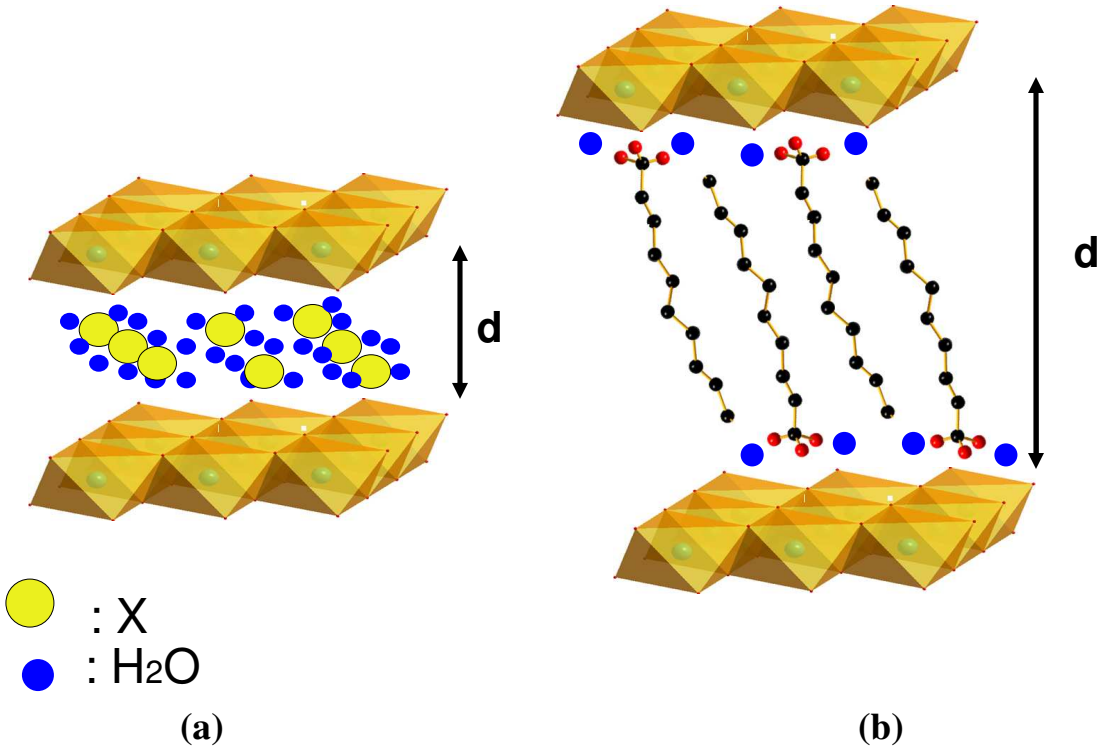

Figure 8: Structural models: **(a)-** Ni-LHS-X hydroxyl-halides deduced from the present structural study and **(b)-** Ni-LHS-$C_nH_{2n}SO_3$ after literature.[33]

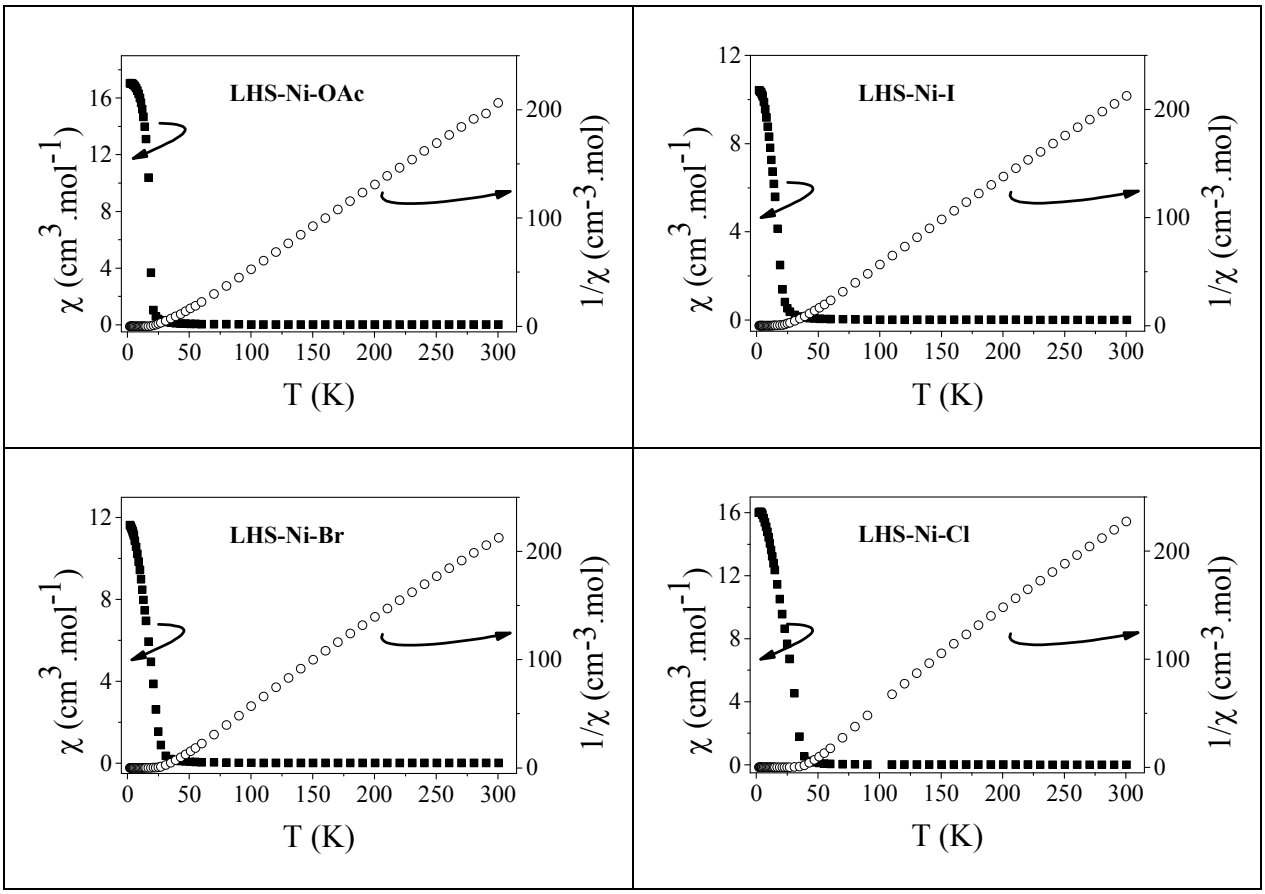

Figure 9: Magnetic DC susceptibility χ and 1/χ versus temperature of nickel hydroxyhalides and hydroxyacetate.

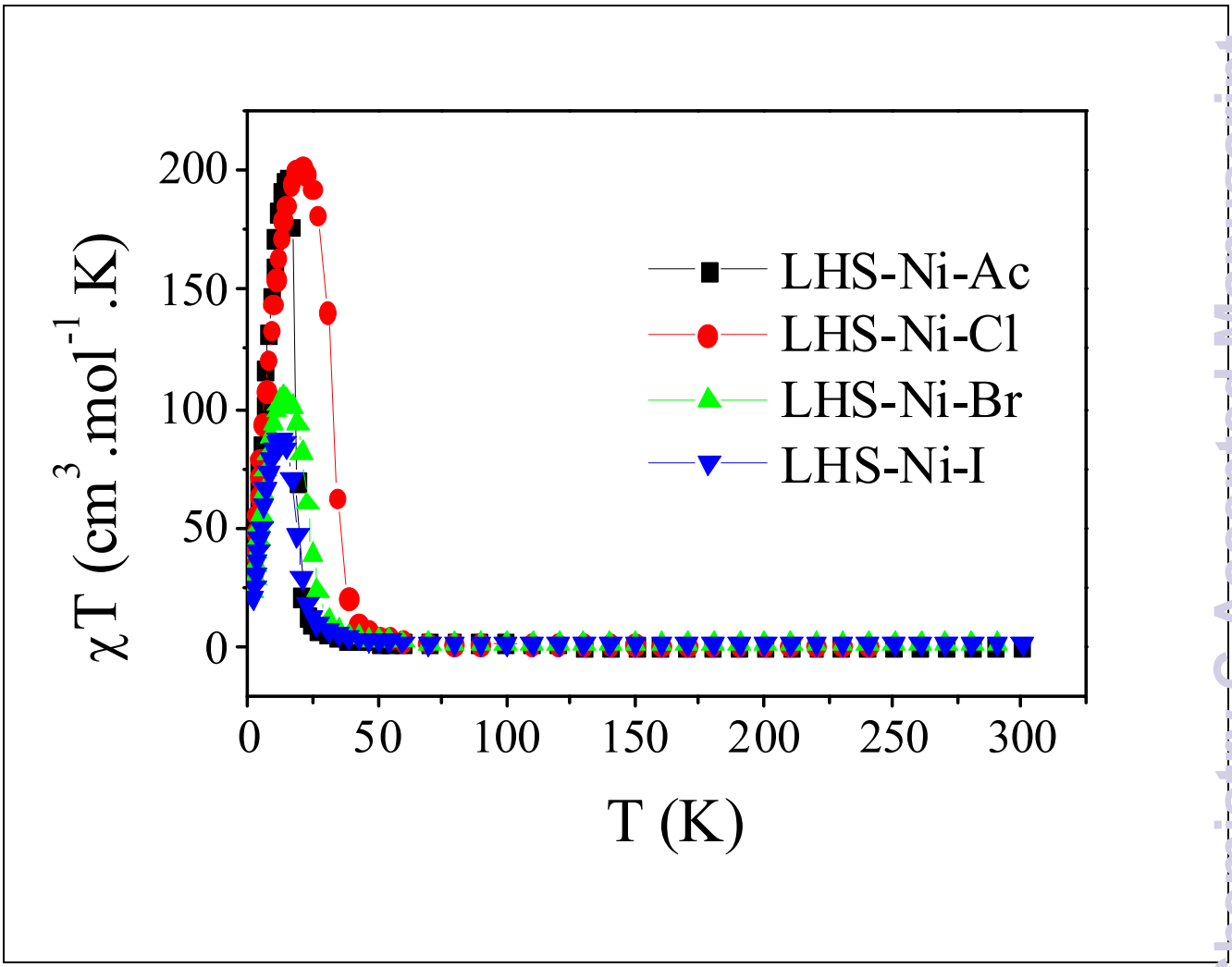

Figure 10: Temperature dependence of the χT product for the three nickel hydroxyhalides and the hydroxyactate in an applied field of 200 Oe.

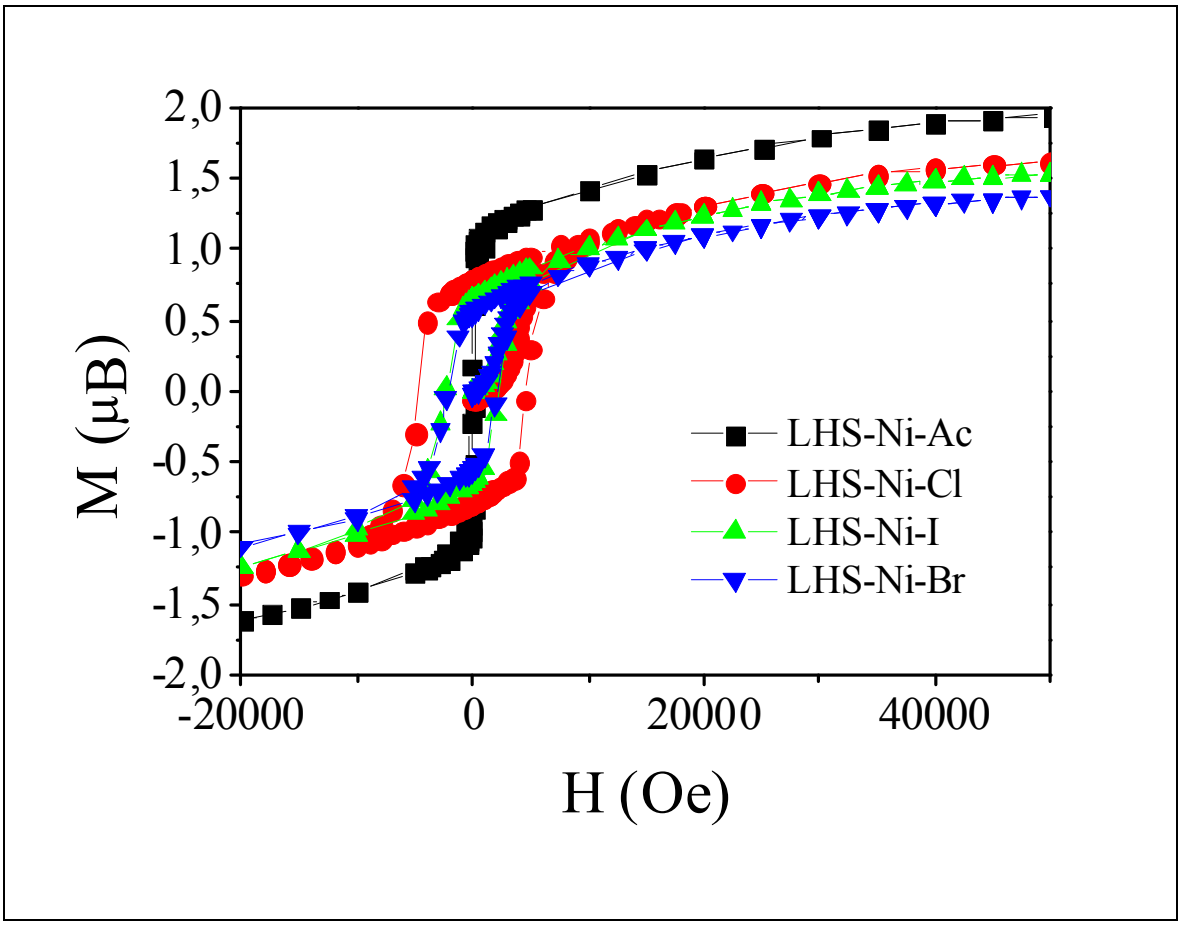

Figure 11: Field-dependence of the magnetization for the nickel hydroxyhalides and the hydroxyacetate at 2 K.

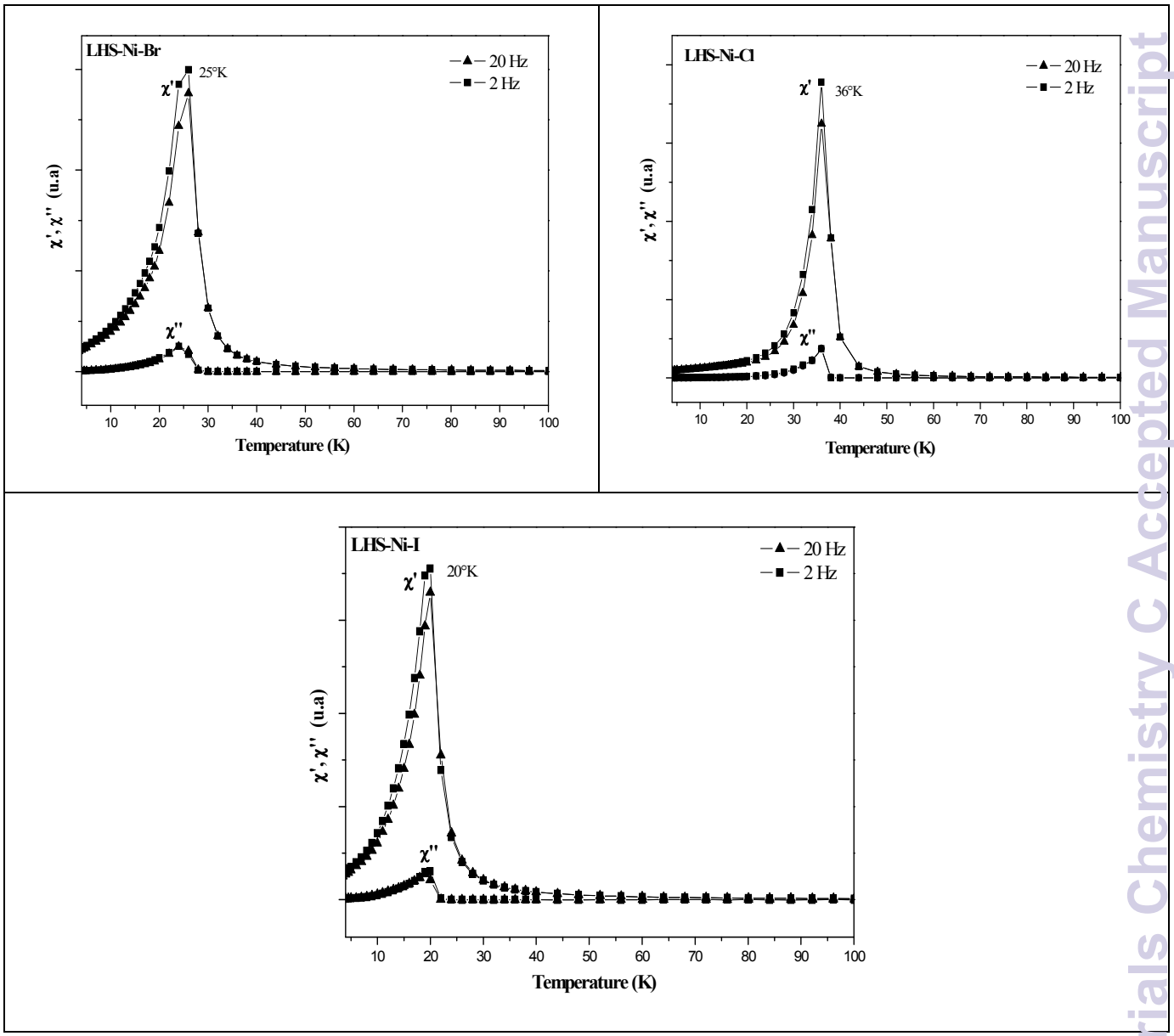

Figure 12: AC susceptibility versus temperature variations of nickel hydroxyhalides.

Table 1: Elemental chemical analysis data, experimental and calculated

Compound	X/Ni[a]	C Weight (%)[b]	H Weight (%)[b]	H_2O Weight (%) [c]	Total weight loss to NiO (%)	
					Exp	Cal
LHS-Ni-Ac	0.51	11.52	3.4	6.6	38.7	41.6
LHS-Ni-I	0.17	1.60	2.7	9.4	39.7	41.3
LHS-Ni-Br	0.16	1.84	2.7	10.6	38.6	37.7
LHS-Ni-Cl	0.17	1.57	2.9	6,7	28.2	30.0

[a] molar ratio; [b] weight percentage from elemental chemical analysis; [c] weight percentage from TG analysis

Table 2: Chemical formula of prepared compounds and amount of polyol (DEG) present in the final products.

Compound	Chemical formula	DEG
LHS-Ni-OAc	$Ni(OH)_{1.49}(CH_3CO_2)_{0.51}.0.46H_2O$	0.052
LHS-Ni-I	$Ni(OH)_{1.83}I_{0.17}.0.64H_2O$	0.041
LHS-Ni-Br	$Ni(OH)_{1.84}Br_{0.16}.0.68H_2O$	0.046
LHS-Ni-Cl	$Ni(OH)_{1.83}Cl_{0.17}.0.40H_2O$	0.035

Table 3: Crystallographic characteristics of prepared compounds

Compound	*a / Å*	*c / Å*	*correlation length according to c axis Å*	*Intensity's ratio I(002)/(I001)*
LHS-Ni-OAc	*3.10 (1)*	*10.53 (6)*	*64*	*0.17*
LHS-Ni-Cl	*3.09 (1)*	*7.93 (7)*	*63*	*0.22*
LHS-Ni-Br	*3.08 (1)*	*8.23 (1)*	*88*	*0.28*
LHS-Ni-I	*3.09 (1)*	*8.60 (2)*	*89*	*0.45*

Table 4: Structural parameter obtained from the EXAFS analysis

Compound	***Neighbours***	***N***	***R / Å***	σ^2*10^3 /Å^2	ΔE_0 / eV
LHS-Ni-OAc	**O**	5.7	2.05	5.8	-4.0
	Ni	6.6	3.10	5.7	-5.7
LHS-Ni-Cl	**O**	6.1	2.05	8.4	-5.0
	Ni	6.7	3.09	9.4	-7.2
LHS-Ni-Br	**O**	5.8	2.05	6.4	-4.7
	Ni	6.6	3.09	7.0	-6.7
LHS-Ni-I	**O**	6.5	2.05	7.2	-4.7
	Ni	6.0	3.08	6.4	-6.9

Table 5: Main magnetic results of prepared compounds

Compound	d/Å	T_c[a] /K	θ_p/K	H_c/Oe	M_s/μ_B at 50 kOe (T = 5 K)	C/cm^3.mol^{-1}.K	g
LHS-Ni-OAc[33]	10.53	17	27	120	1.88 (T = 2K)	1.32	2.3
LHS-Ni-Cl	7.93	36	23	120	1.50	1.20	2.2
LHS -Ni-Br	8.23	25	16	480	1.66	1.33	2.3
LHS-Ni-I	8.60	20	19	150	1.76	1.32	2.3
LHS-Ni-$C_{10}SO_3$[33]	22.77	17	11	240	1.36	1.20	2.2
LHS-Ni-$C_{l4}SO_3$[33]	26.79	17	15	1990	1.54	1.20	2.2
LHS-Ni-$C_{18}SO_3$[33]	31.88	17	11	2310	1.72	1.4	2.4

[a] value measured at the maximum of χ' (T).

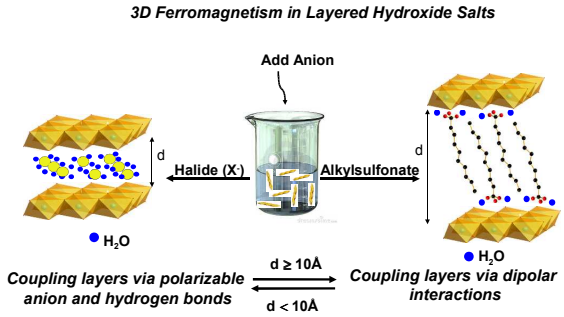

The structural and magnetic investigation of the new Nickel-layered hydroxy-halides LHS-Ni-X (X = Cl, Br, I) gives new insight on the magnetic interaction mechanisms in the two-dimensional α-$Ni(OH)_2$ systems.